Journal of Catalysis **200,** 377–388 (2000)
doi:10.1006/jcat.2001.3222, available online at http://www.idealibrary.com on IDEAL®

Continuous Enantioselective Hydrogenation of Ethyl Pyruvate in "Supercritical" Ethane: Relation between Phase Behavior and Catalytic Performance

R. Wandeler, N. Künzle, M. S. Schneider, T. Mallat, and A. Baiker[1]

Laboratory of Technical Chemistry, Swiss Federal Institute of Technology, ETH Zentrum, CH-8092 Zürich, Switzerland

Received November 27, 2000; revised January 26, 2001; accepted February 26, 2001; published online May 15, 2001

Continuous hydrogenation of an α-ketoester has been studied in a fixed-bed reactor over cinchonidine-modified Pt/Al_2O_3 using "supercritical" ethane as a solvent. Application of ethane as a solvent offers good enantioselectivity and very fast conversion of ethyl pyruvate to ethyl lactate (average turnover frequency of 15 s^{-1} at ambient temperature). The phase behavior in the temperature range 15–50°C and at pressures up to 140 bar has been investigated in a computer-controlled view cell, equipped with on-line video imaging and recording. The changes in reaction rate and enantioselectivity with pressure (density), temperature, and hydrogen concentration are interpreted by considering the number and nature of phases present under the conditions applied. The results illustrate the obvious limitations of describing multicomponent phase behavior with that of the pure solvent. We demonstrate that consideration of the phase behavior of a binary fluid system is an ideal guide for rationalizing the phase behavior-related phenomena typical of multicomponent high-pressure reaction systems.

Key Words: **enantioselectivity; hydrogenation; ethyl pyruvate; α-ketoester; supercritical ethane; high-pressure reactions; binary mixture; phase diagram; fluid equilibrium.**

INTRODUCTION

Application of supercritical fluids (SCFs) as solvents and reactants attracts growing interest in both homogeneous (1–4) and heterogeneous (4–6) catalysis. Near the conditions where two phases critically merge, fluids reveal striking phenomena: some physical properties exhibit major tunability, with possible discontinuity or divergence, and fluctuations in density or concentrations lead to critical opalescence (7). At temperatures above the critical value, however, supercritical fluids lose these almost magic "critical" properties; yet, they reveal a unique combination of gas-like and liquid-like qualities due to their intermediate molecular density, which renders them interesting media for chemical processes (8).

[1] To whom correspondence should be addressed. Fax: +41 1 632 11 63. E-mail: baiker@tech.chem.ethz.ch.

Most "supercritical" reactions are conducted far from a critical point (9); still, the special effects observed in rate and selectivity are often traced to a "critical" phenomenon, mostly a change from a two-phase to a one-phase system. Although the importance of phase behavior in high-pressure systems is generally accepted, the complexity of high-pressure multicomponent systems is often underestimated. Even if the number and nature of phases present in a reaction mixture is investigated experimentally, assumption of a phase behavior similar to that of a pure fluid is quite common. Typical phenomena inherent to multicomponent systems are, e.g., coexisting phases with different composition, fluid–fluid immiscibilities, and related discontinuities of critical lines (10). Disregarding these phenomena may lead to a false interpretation of the observed effects in high-pressure chemistry. Note that the widely used term *supercritical* is deprived of any meaning in multicomponent systems since phase separation is still possible at conditions beyond the mixture critical point ("retrograde condensation" (10, 11)) or the critical points of the pure components ("gas–gas immiscibility" (10)). For convenience, the term "supercritical" ("sc") is used here in quotes for a dense fluid phase at temperatures exceeding its mixture critical point, irrespective of further liquid phases present.

Heterogeneously catalyzed continuous hydrogenations in supercritical solvents have been reported for a variety of substrates (4–6); however, only chemoselective hydrogenations have been studied. We propose that enantioselective hydrogenations are well-suited test reactions to explore the interrelation between phase behavior and catalytic performance due to their high sensitivity to the reaction medium.

Here we report the continuous enantioselective hydrogenation of ethyl pyruvate (EP, Scheme 1) in "supercritical" ethane ($p_c = 48$ bar, $T_c = 32$°C). Ethyl pyruvate hydrogenation over cinchonidine (CD)-modified Pt is the most studied example of α-ketoester hydrogenation (12–22), affording up to 97.5% enantioselectivity (ee) under carefully optimized conditions (23, 24). Enantioselective hydrogenation of EP in "supercritical" ethane and CO_2 has already been investigated in a batch reactor (25), and more recently in

0021-9517/01 $35.00

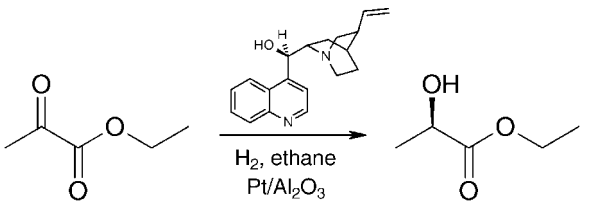

SCHEME 1. Enantioselective hydrogenation of ethyl pyruvate over cinchonidine (CD)-modified Pt/Al_2O_3 to afford (*R*)-ethyl lactate.

a flow reactor (26) showing that "sc" ethane in a superior reaction medium. This preliminary studies did not include a detailed analysis of the phase behavior under reaction conditions.

EXPERIMENTAL METHODS

Phase Behavior Studies

The phase behavior of the system under reaction conditions was investigated in a computer-controlled high-pressure view cell of variable volume (23–63 ml), equipped with on-line digital video imaging and recording. A flowchart of the view cell setup is given in Fig. 1.

The magnetically stirred cell consists of a horizontal cylinder equipped with a sapphire window covering the entire diameter (26 mm) and an opposite, horizontally moving piston equipped with another sapphire window for illumination of the system. The cell is custom-designed starting from a commercial screw-type manual pump (SITEC Sieber Engineering AG, Switzerland). The setup of the view cell allows the observation of even minor volumes of gaseous and liquid phases and thus facilitates reliable static measurements of equilibria using the synthetic method (27).

The view cell is designed for experiments in the temperature range −20 to 200°C and at pressures up to 200 bar. The sapphire windows at the front and back of the cell are sealed using a PTFE O-ring and a direct metal–sapphire sealing, respectively. The moving piston is sealed with a combination of a PTFE/carbon–PTFE Bridgman sealing and a PTFE O-ring. The variable volume of the view cell is measured with a displacement transducer (Genge & Thoma HP 22 CP) monitoring the position of the moving piston. Temperature is controlled with an oil-containing heating jacket and a combined thermo-/cryostat (Julabo F25 HD). Temperature is measured with a Type J thermocouple with on-board cold-junction temperature compensation. Pressure is measured with a pressure transmitter with integrated amplifier for high temperature and pressure (Dynisco MDT422H-1/2-2C-15/46) to allow reliable pressure measurements over a broad temperature range at low stagnant volume. The view cell is equipped with a magnetic stirrer (Heidolph MR 2002) for mixing and a system of automated valves (SITEC Sieber Engineering AG,

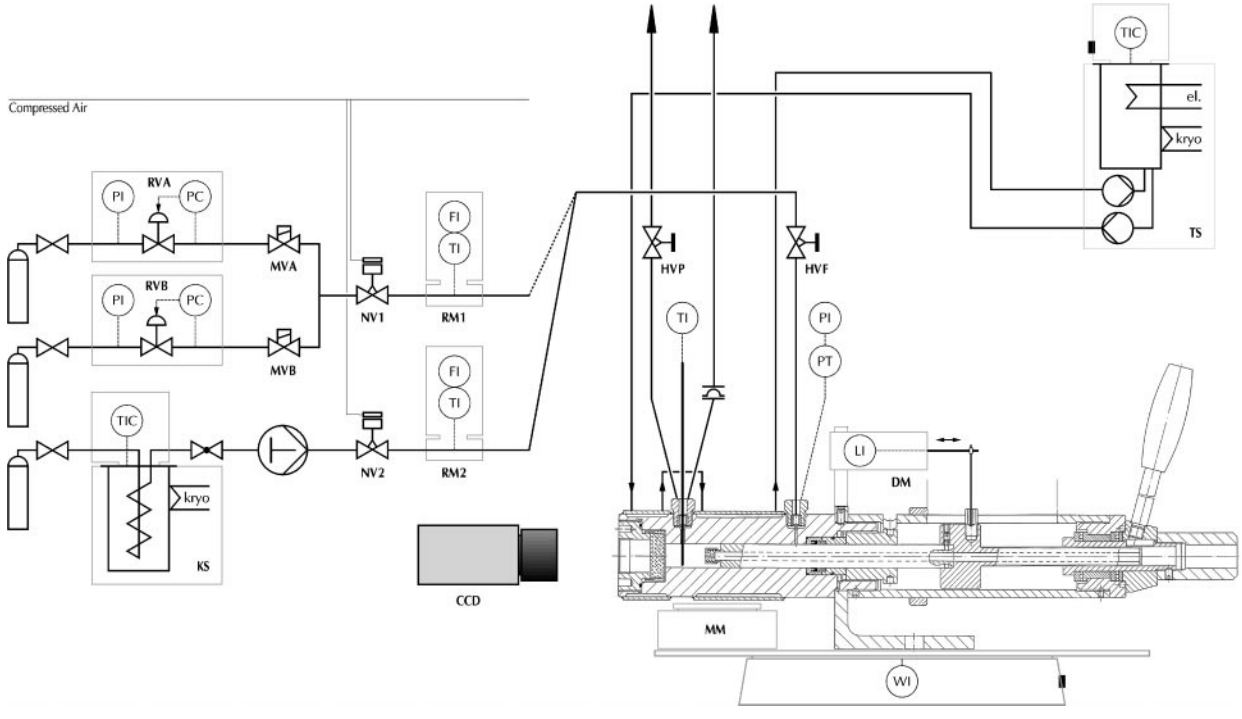

FIG. 1. Flowchart of the high-pressure view cell including the organization of process control and acquisition of data and images. PI, pressure indicator; PT, pressure transducer; TI, temperature indicator; TIC, temperature controller; FI, flow indicator; LI, length indicator; WI, weight indicator; RVx, high-pressure reduction valves; MVx, magnetic valves; NVx, needle valves; HVF/HVP, manual needle valves for cell filling and purge, respectively; RMx, mass-flow meter; MM, magnetic mixer; DM, displacement transducer; KS, cryostat; TS, thermostat; CCD, 8-bit monochrome CCD camera.

Switzerland), automated needle valves (Kämmer Ventile, Germany), manual needle valves (SITEC Sieber Engineering AG, Switzerland), and mass-flow meters (Rheonik Messgeräte GmbH, Germany) for adding fluids into the system as well as purging the reactor contents after an experiment. Filling of the view cell can be double-checked with the help of a balance (Mettler Toledo SG32001), on which the view cell is mounted self-supportingly.

The phase behavior has been monitored by on-line video imaging with a system developed in cooperation with Videal AG, Switzerland. The view cell can be illuminated with visible light of variable wavelength and intensity. The light is supplied by a cold light source with corresponding filters via optical fibers and a sapphire window at the back of the cell. The analogue video signal transmitted by a monochrome 8-bit CCD camera (Kappa CF 8/4) is recorded digitally (Panasonic DVCPro AJ-D230). The very sensitive camera shows turbulences and differences in phase densities that are hardly visible without optical aids, rendering the observation by on-line video imaging very accurate.

The view cell is operated using a computer-based approach for temperature control, data acquisition and processing, image acquisition, and mixing. Changes in the view cell's volume as well as in dosing of components were induced manually. Analogue input and output signals, as well as digital I/O, are handled by two 16-bit, 20 kS/s AT and PCI data acquisition boards (NI AT/PCI-MIO-16XE-50) via corresponding connector boards with on-board cold-junction temperature compensation for the thermocouple and relays. Serial communication with the thermostat, balance, and digital video recorder is managed by an ISA four-port board (NI AT-4-RS232). The analogue monochrome video signal is captured using a monochrome image acquisition board (NI IMAQ PCI-1408).

Software for control of the view cell was developed using National Instruments (NI) BridgeVIEW on a Windows NT-based 300-MHz Pentium II computer. The approach in design of the software solution is similar to that of a high-pressure batch system for *in situ* monitoring of heterogeneously catalyzed reactions reported in detail elsewhere (28, 29).

Catalytic Hydrogenation

Catalytic studies were carried out in a continuous stainless-steel tubular fixed-bed reactor of 12.5-mm inner diameter, equipped with either an electric heating or a cooling jacket. The reaction temperature was monitored with an adjustable thermocouple inside the catalyst bed. Constant pressure was maintained with a pressure controller (NWA).

A mechanical mixture of 100 mg 5 wt% Pt/Al_2O_3 (Engelhard 4759) and 900 mg Al_2O_3 as diluent was employed, resulting in a catalyst bed length of 15 mm. The particle size of the catalyst was 25–250 μm. Alumina was used as diluent to prevent full conversion of EP at the flow rates chosen; the catalytic studies thus aimed at clarifying the influence of the phase behavior on the rate and selectivity, rather than optimal usage of the continuous reactor. The catalyst was pretreated at 400°C by flushing with 12 ml min^{-1} N_2 (99.995%) for 30 min, followed by a reductive treatment in H_2 (99.999%) for 90 min. After being cooled to room temperature in H_2, the catalyst was immediately transferred to the reactor. It has been shown that high-temperature pretreatment of Pt/alumina in H_2 can double the ee, and exposure to ambient air after the reductive treatment has no significant influence on the catalyst performance (30).

The reaction was conducted at a molar ethane : EP : H_2 ratio of 200 : 1 : k, where k was 2, 10, or 20. A flow of 1.0 ml min^{-1} EP (Fluka, 97%) was mixed with ethane (99.5%) and H_2 (99.999%) in a static mixer before entering the reactor. CD (Fluka, >98%) was fed together with EP at a molar CD : EP ratio of 1 : 2500. The corresponding solution was prepared immediately before the reaction and kept cool and in the dark to minimize side reactions (31). EP/CD and ethane were continuously fed into the reactor with an HPLC pump (Gilson M305). Note that minor amounts of chiral modifier have to be fed continuously into the reactor to maintain the good ee with time-on-stream (32). The ethane flow was kept constant by a two-step expansion valve (NWA PE103) and monitored with a rotameter. H_2 was continuously fed into the reactor by a six-port valve.

Conversion and ee were determined without derivatization with an HP 5890A gas chromatograph and a chiral capillary column (WCOT fused silica 25 m × 0.25 mm, coating CP Chiralsil-Dex CB, Chrompack). Enantioselectivity is expressed as ee (%) = R (%) − S (%). The ca. 1% racemic ethyl lactate impurity in EP was taken into consideration. Turnover frequency (TOF) is related to the number of surface Pt sites; Pt dispersion after heat treatment was 0.27 (33). Chemoselectivity to ethyl lactate was always 100%.

RESULTS

Phase Behavior

The phase behavior of the reaction mixture is characterized by the four basic isobaric phase equilibrium transitions shown in Fig. 2: (i) At 20°C and low H_2 concentrations, the system consisted of a liquid EP-rich phase in equilibrium with a gaseous ethane-rich phase at low pressures. With increasing pressure the amount of liquid increased, resulting in an equilibrium of a homogeneous liquid EP/ethane phase with a gaseous ethane-rich phase at medium pressures, and a liquid EP/ethane single phase with dissolved H_2 at higher pressures. At medium pressures and higher H_2 concentrations, a gaseous H_2-rich phase persisted in equilibrium with the homogeneous liquid EP/ethane phase, saturated with H_2. (ii) At 30°C, the system consisted of a

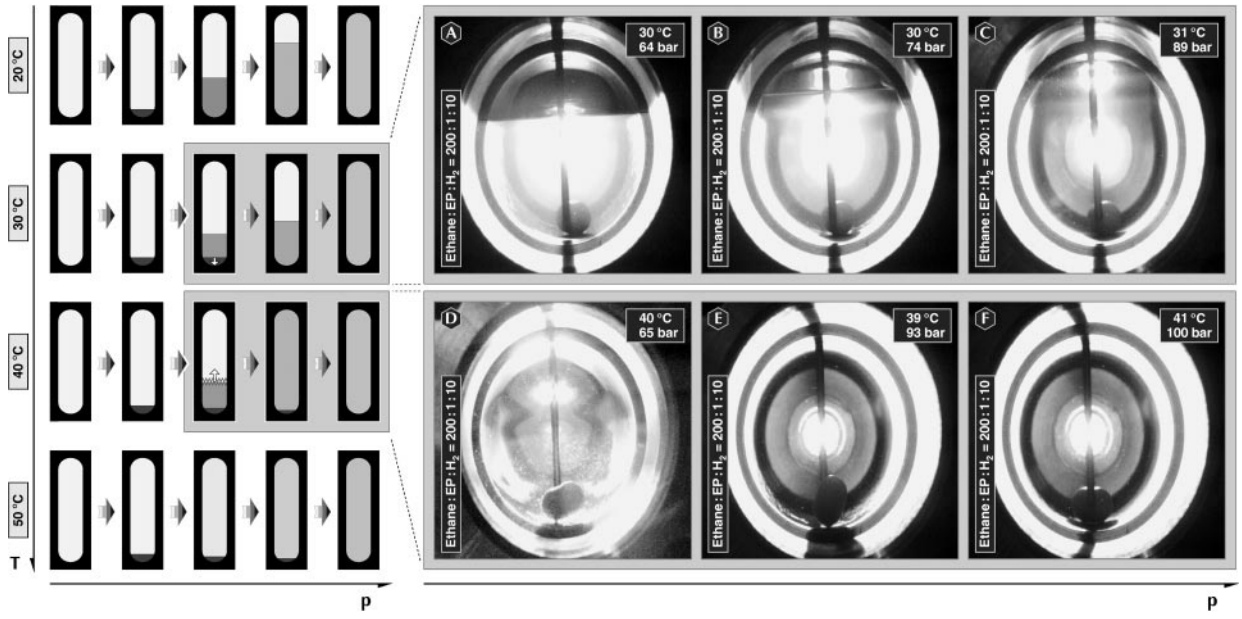

FIG. 2. Phase behavior in the system ethane : EP : H_2 as a function of pressure and temperature for a molar ratio of 200 : 1 : 10. The phase transitions in the shaded area are illustrated by snapshots A–F on the right. 20°C: liquid EP and ethane fully miscible, leading to a "conventional" transition from a gaseous system at low pressures to a liquid system at high pressures by way of a two-phase region. 30°C: liquid EP and ethane only partially miscible; condensation of an EP-rich liquid phase at low pressures and an additional ethane-rich liquid phase as pressure is increased, leading to a liquid–liquid–vapor equilibrium; a further increase in pressure leads to a two-phase equilibrium of ethane-rich phases and, finally, to a single liquid phase. 40°C: same behavior as at 30°C up to the liquid–liquid–vapor equilibrium; further increase in pressure leads to an equilibrium of the liquid EP-rich phase and a dense ethane-rich phase, with either the gaseous ethane-rich phase disappearing or critically merging with the liquid ethane-rich phase (at temperatures slightly above 40°C) as pressure is increased. 50°C: Condensation of an EP-rich liquid phase in equilibrium with a gas-like "sc" ethane-rich phase; transition to a single-phase system with increasing pressure. The bright round spot at the opposite end of the cell is the sapphire window used for illumination; the outer white circle is caused by reflection of light at the outer flange of the sapphire window; the vertical thermocouple and PTFE magnetic stirrer at the bottom of the cell are visible.

liquid EP-rich phase in equilibrium with a gaseous ethane-rich phase at low pressures. With increasing pressure the system went through a three-phase LLV equilibrium (EP-rich liquid, ethane-rich liquid, and ethane/H_2-rich gaseous phase) at around 50 bar, before changing to an equilibrium of a homogeneous liquid EP/ethane phase in equilibrium with a gaseous ethane/H_2-rich phase. (iii) At 40°C, the system consisted of a liquid EP-rich phase in equilibrium with a gaseous ethane-rich phase at low pressures. With increasing pressure, the system again went through a three-phase LLV equilibrium (EP-rich liquid, ethane-rich liquid, and ethane/H_2-rich gaseous phase, see Fig. 3G) whereby the upper two ethane-rich phases critically merged in the vicinity of 40°C and 70 bar in an upper critical endpoint (UCEP), as shown in Figs. 2D and 3H. Further increase in pressure led to an equilibrium of a liquid EP-rich phase and a "sc" ethane-rich phase at first with decreasing amount of liquid and finally to a single-phase system. (iv) At 50°C, i.e., beyond the upper critical endpoint of the coexistence of the ethane-rich phases, the system exhibited a two-phase equilibrium of a liquid EP-rich phase and a dense fluid ("sc") ethane-rich phase, continuously blending into one phase at higher pressures.

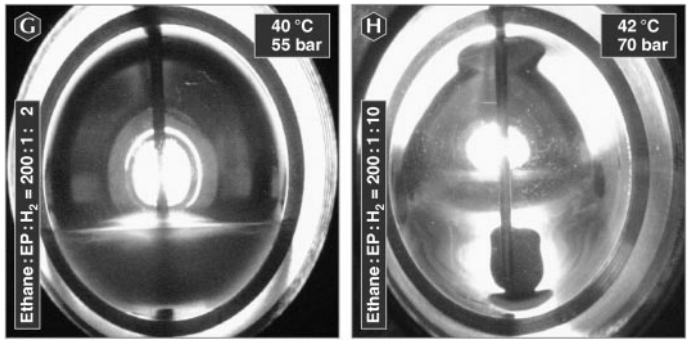

FIG. 3. Interlaced video image of the view cell showing the phase behavior of two ethane/EP/H_2 mixtures at around 40°C. (G) Three-phase liquid–liquid–vapor equilibrium at 55 bar. (H) Critical merging of the upper two ethane-rich phases at 70 bar, leading to an equilibrium of a "supercritical" ethane-rich phase and a liquid EP-rich phase. The bright round spot at the opposite end of the cell is the sapphire window used for illumination; the outer white circle is caused by reflection of light at the outer flange of the sapphire window; the vertical thermocouple and magnetic stirrer at the bottom of the cell are visible.

The number and nature of phases at a given temperature and pressure depended strongly on H_2 concentration. Accordingly, the pressure required for transition to a single-phase system increased remarkably with temperature and H_2 concentration in the system, as illustrated in Fig. 4.

Measurements with different compositions (Fig. 5), corresponding to reaction mixtures at conversions of 0, 50, and 100%, showed that the overall density (which is crucial for phase behavior) does not change significantly with conversion in the entire temperature and pressure ranges investigated.

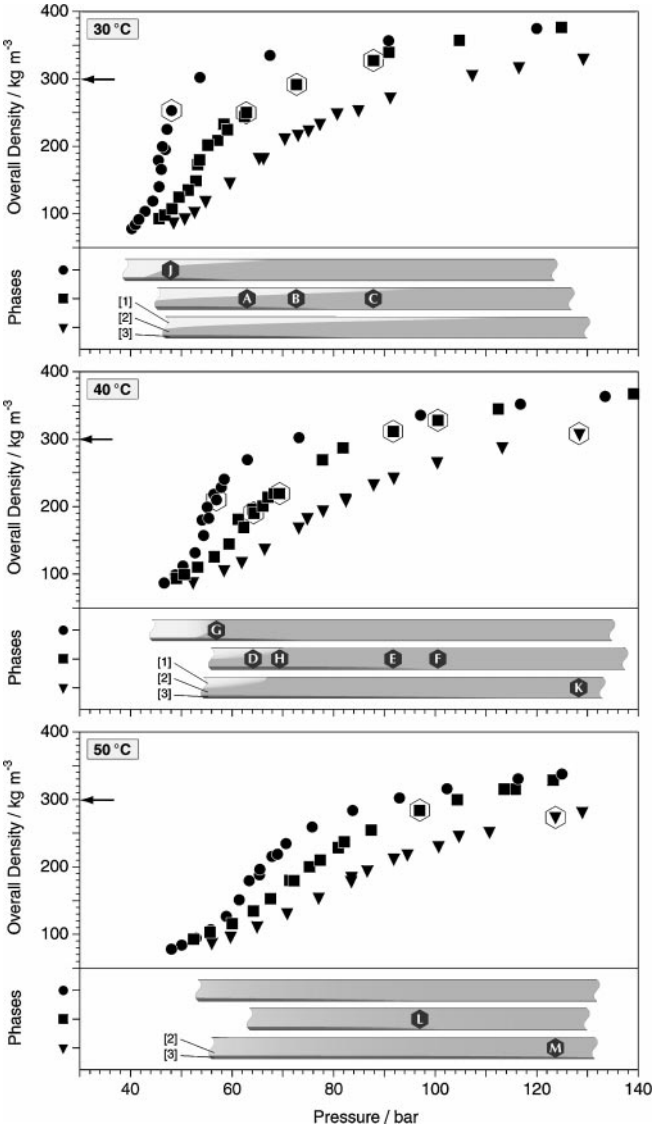

FIG. 4. Influence of pressure and H_2 concentration on the overall density and phase behavior of the reaction mixture for 30, 40, and 50°C. Ethane : EP : H_2 molar ratio = 200 : 1 : k, where (●) $k = 2$, (■) $k = 10$, (▼) $k = 20$. Phases: [1] gaseous, ethane/H_2-rich phase; [2] dense fluid, ethane-rich phase; [3] liquid, EP-rich phase. Arrow indicates the density required to reach the one-phase region. Note the significant increase in pressure required to reach this density with increasing temperature and H_2 concentration. The hexagons mark and label the corresponding snapshots in Figs. 2, 3, 11, and 13.

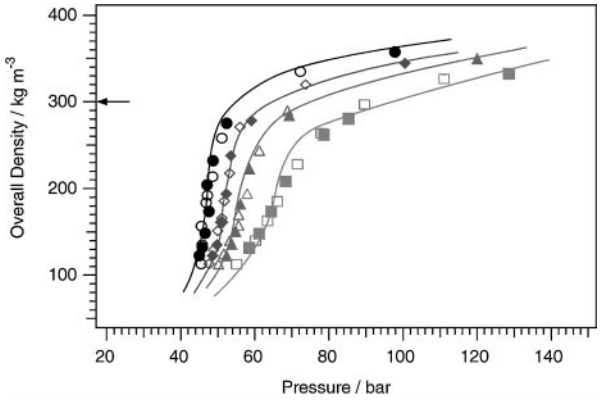

FIG. 5. Comparison of three different compositions, corresponding to reaction mixtures at conversions of 0% (line), 50% (open symbols), and 100% (filled symbols) with a molar ratio of ethane : (EP + EL) : H_2 = 200 : 1 : 2 at various temperatures (30°C, 35°C, 40°C, 50°C from black to light gray). Arrow indicates the density required to reach the one-phase region.

The CD concentration in the reaction mixture was more than an order of magnitude lower than the impurity level of EP. Hence we assumed that the effect of CD on the phase behavior is negligible and that the system can be well represented by the ethane/EP/H_2 mixture discussed above.

Catalytic Studies

At low and medium temperatures the conversion of EP to ethyl lactate increased with pressure, as illustrated in Fig. 6 for the reaction at 40°C. Interestingly, the conversion

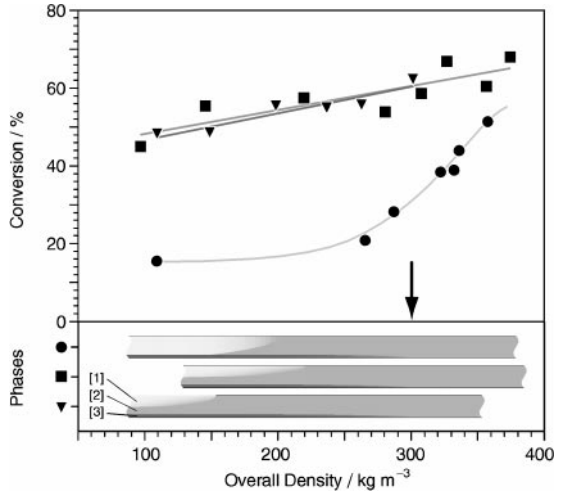

FIG. 6. Conversion of EP (top) and phase behavior of the reaction mixture (bottom) at 40°C as a function of overall density at various H_2 concentrations. Ethane : EP : H_2 molar ratio = 200 : 1 : k, where (●) k = 2, (■) $k = 10$, (▼) $k = 20$. Phases: [1] gaseous, ethane/H_2-rich phase; [2] dense fluid, ethane-rich phase; [3] liquid, EP-rich phase. Arrow indicates the density required to reach the one-phase region.

changed continuously with density at higher H_2 concentrations, irrespective of changes in phase behavior. In contrast, at low H_2 concentration the appearance of one single phase was accompanied by a pronounced rate enhancement.

Whereas the rate enhancement with increasing pressure persisted at 50°C for low H_2 concentration, high H_2 concentrations resulted in a slightly falling tendency in EP conversion. Figure 7a shows a comparison of EP conversion at 30 and 50°C for high H_2 concentration, clearly exemplifying the transition of a positive influence of pressure on the reaction rate at lower temperature to a negative effect at 50°C.

At high pressures, conversions in the range 40–70% were found for all temperatures and H_2 concentrations (at the mass-flow rates applied). The maximum conversion decreased slightly with increasing temperature. Interestingly,

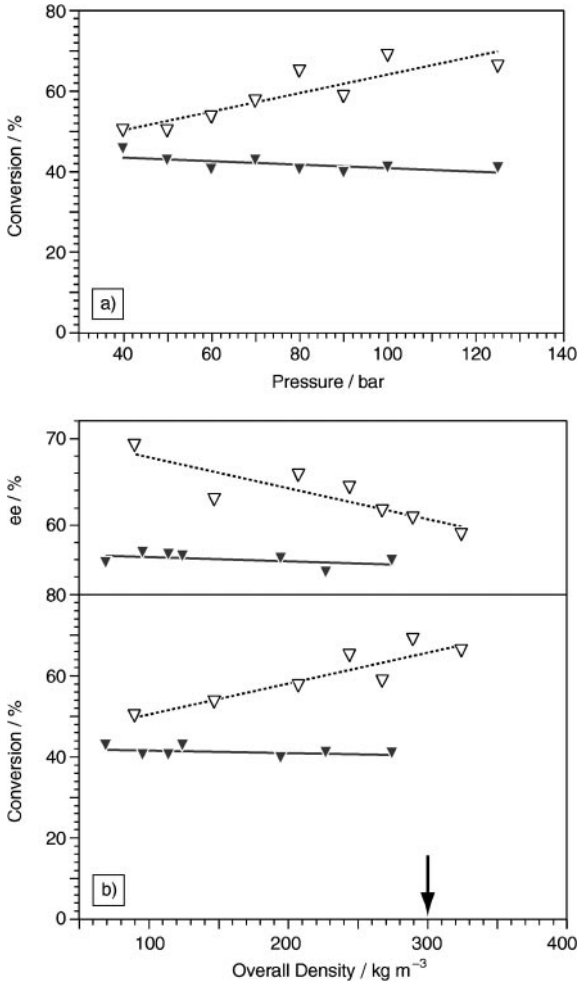

FIG. 7. Typical examples of the changes in enantioselectivity and conversion with temperature and overall density or pressure. Ethane : EP : H_2 molar ratio 200 : 1 : 20. (▽) 30°C; (▼) 50°C. (a) Influence of pressure on the conversion of EP. (b) Enantioselectivity (top) and conversion of EP (bottom) as a function of overall density. Arrow indicates the density required to reach the one-phase region.

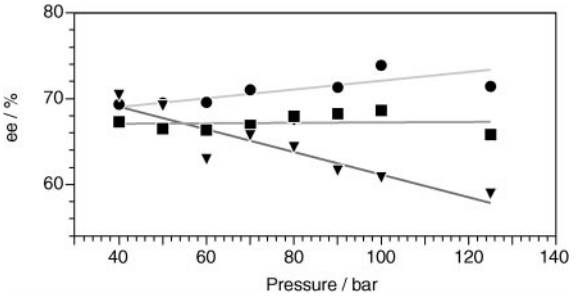

FIG. 8. Influence of pressure and H_2 concentration on the enantioselectivity at 30°C. Ethane : EP : H_2 molar ratio = 200 : 1 : k, where (●) k = 2, (■) k = 10, (▼) k = 20.

at 50°C and pressures exceeding 70 bar, highest conversion was obtained at a molar EP : H_2 ratio of 1 : 10. Doubling the H_2 concentration resulted in a lower conversion by 20%.

Enantioselectivity to (*R*)-ethyl lactate was found to exhibit rising, constant, and falling tendency with increasing total pressure, depending on the temperature and H_2 concentration. Some examples are collected in Fig. 8. Rising ee with pressure was observed at low temperature and H_2 concentration, shifting to a decreasing tendency with increasing temperature and H_2 concentration. For most conditions, the ee varied smoothly, almost linearly, with pressure, despite evident changes in the phase behavior (Fig. 4). Since increasing pressure generally resulted in higher conversion, the enantioselectivity exhibited similar trends with increasing conversion and pressure (Fig. 9). Under certain conditions, however, a change from a rising to a falling trend with increasing conversion could be identified (Fig. 9, 50°C). Another intriguing observation is that at low temperature and high H_2 concentration the ee dropped by ca. 10% in a narrow conversion range of 20% (Fig. 9). For comparison, in conventional organic solvents the variation of ee with conversion is minor, except the tendency to rise in the initial transient period when impurities are present (34).

Experiments carried out in the temperature range 35 to 140°C revealed an interesting behavior of reaction rate and ee (Fig. 10). The decline in ee at higher temperature is

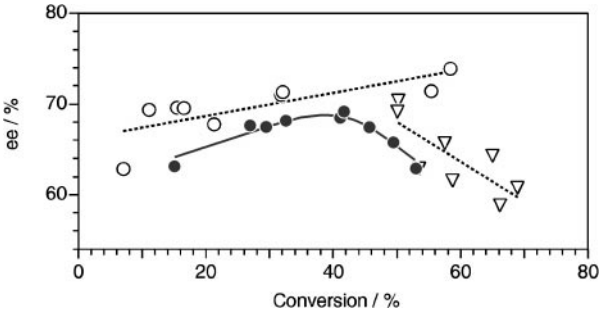

FIG. 9. Enantioselectivity as a function of EP conversion. Ethane : EP : H_2 molar ratio = 200 : 1 : 2, (○) 30°C, (●) 50°C; Ethane : EP : H_2 molar ratio = 200 : 1 : 20, (▽) 30°C.

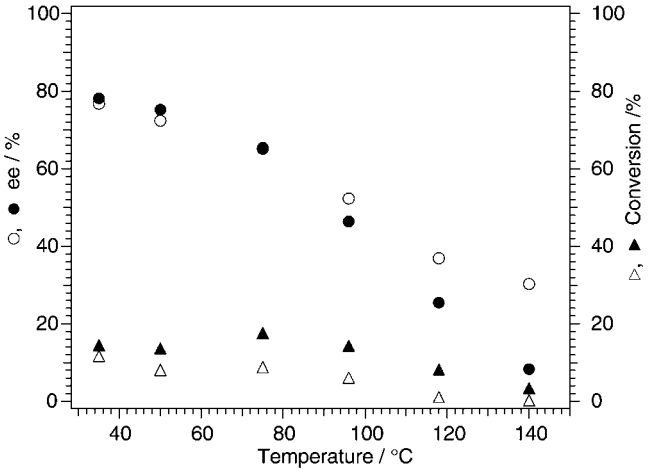

FIG. 10. Influence of temperature on conversion and ee in the hydrogenation of EP at 100 bar and molar ethane : EP : H_2 ratios of 200 : 1 : k. Open symbols: $k = 2$, filled symbols: $k = 20$. Catalyst amount was 10 times lower than under standard conditions.

probably due to a change in the adsorption mode of CD. Assuming that the adsorption mode changes from adsorption via the quinoline ring (parallel to the Pt surface) to tilted adsorption (35), it can be inferred that at higher temperature the modifier no longer adopts the appropriate adsorption geometry for the enantio-discriminating interaction with EP (21, 22).

The weak dependence of reaction rate on temperature can be explained by the two counteracting factors: (i) enhancement of rate with increasing temperature, and (ii) loss of ligand acceleration effect at higher temperature due to inappropriate anchoring of the modifier. Another factor influencing the dependence of reaction rate and ee on temperature could be partial hydrogenation of the quinoline moiety which is expected to be more pronounced at higher H_2 concentration (36). Although experiments were performed at two different hydrogen concentrations the results cannot give a conclusive answer to which of the factors discussed is more important.

Finally, it should be stressed, that the continuous enantioselective hydrogenation in "supercritical" ethane afforded remarkably fast reaction with good ee. At best, a TOF of 15 s^{-1} at 70% conversion was obtained at 25°C. In comparison, using toluene as a solvent at ambient temperature provided a TOF of 1.8 s^{-1} under otherwise comparable conditions and optimal H_2 concentration.

DISCUSSION

Phase Behavior of the Reaction System

The reaction system exhibited a diverse phase behavior in the parameter range considered. Liquid ethane and EP exhibited only partial miscibility at temperatures exceeding ca. 25°C, while being fully miscible at lower temperatures (verified down to 15°C) at the molar ethane : EP ratio of 200 : 1 considered here. Figure 11 illustrates this change in EP solubility in the region of coexistence of a liquid and gaseous ethane-rich phase, i.e., separation of a liquid EP-rich phase at higher temperature for a system with low H_2 concentration.

The solubility of EP in the ethane-rich dense phase is expected to depend mainly on the density of this phase in the temperature range investigated (37). In fact, complete solvation of EP occurred at a density of around 300 kg m^{-3} for all temperatures and H_2 concentrations applied, resulting in a saturated ethane-rich dense phase under these conditions. Figure 4 shows that the higher the H_2 concentration in the system, the higher is the pressure required to achieve a density of 300 kg m^{-3} and thus complete solubility of EP in the dense ethane-rich phase. Note that this isochoric pressure effect of H_2 exceeds significantly the pressure increase that can be expected assuming ideal gas behavior, independent of the number of phases present. As illustrated in Fig. 12, this deviation from ideal behavior became more pronounced with increasing pressure, due to interaction of H_2 with the dense phase(s). This phenomenon is not surprising under the conditions applied. However, it questions the common practice in high-pressure hydrogenations when interpreting the influence of H_2 "partial pressure" on the catalyst performance.

The major influence of temperature and H_2 concentration on the pressure required to obtain a single-phase system is illustrated in Fig. 13. The matrix in temperature and H_2 concentration shows the condensation of a new EP-rich liquid phase from the single-phase reaction mixture via an isoplethic increase in temperature, or an isothermal increase in H_2 concentration, at temperatures and pressures well above the critical values of the pure solvent (ethane, $T_c = 32.2$°C, $p_c = 48.8$ bar). This striking observation

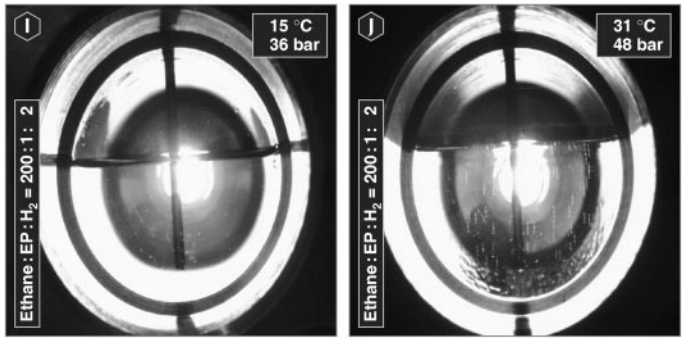

FIG. 11. Interlaced video image of the view cell showing the phase behavior of an ethane : EP : H_2 mixture with 200 : 1 : 2 molar ratio. (I) 15°C; EP is completely soluble in the liquid ethane-rich phase. (J) 31°C, during expansion; liquid EP and ethane are partially immiscible (three-phase liquid–liquid–vapor equilibrium with a thin film of a liquid EP-rich phase at the bottom of the cell); note the emerging gas bubbles (H_2) in the liquid ethane-rich phase during expansion. For an explanation, of the general features of the snapshots cf. Fig. 3.

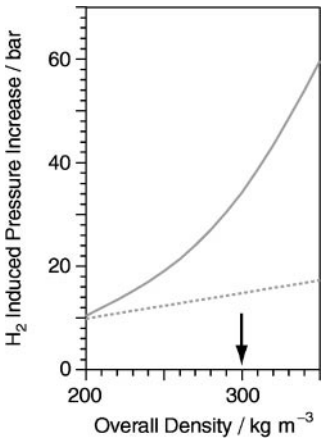

FIG. 12. Pressure increase induced by isochoric addition of H_2 to a mixture of ethane and EP at 40°C, leading to a mixture with a molar ethane : EP : H_2 ratio of 200 : 1 : 10 as a function of the overall density of the ethane/EP mixture. Full line : H_2-induced pressure increase as measured; dashed line: pressure increase as expected from ideal gas behavior. Arrow indicates the density required to reach the one-phase region.

demonstrates the danger of assuming that the phase behavior of a multicomponent system is similar to that of the pure solvent—another practice often encountered in interpreting reactions in "supercritical" solvents.

Solubility of H_2 in the liquid phases decreased with increasing temperature and decreasing pressure. The pressure effect on H_2 solubility in the ethane-rich liquid phase is illustrated in Fig. 11(J), where emerging gas bubbles on expanding the system are clearly visible.

These observations illustrate the influence of temperature, pressure, and H_2 concentration not only on the number and nature of phases present in the reaction mixture, but also on their composition. Phase behavior, comprising the composition of phases present in the system, does inevitably vary with changes of the reaction parameters. These variations should therefore be considered throughout the process for an unequivocal interpretation of the differences in rate and selectivity of the reaction.

Modeling Phase Behavior with a Binary Fluid Mixture

The fact that coexisting phases are in general of different composition, and the possibility of fluid–fluid immiscibilities and related discontinuities of critical lines, render phase diagram topologies of multicomponent systems rather complex. Since these phenomena do not occur with pure fluids, multicomponent phase behavior cannot satisfactorily be approximated by the simple topology of a pure fluid phase diagram. On the other hand, a detailed consideration of the real multicomponent system, in our case ethane/H_2/EP/ethyl lactate/CD, is of questionable value in a discussion of high-pressure reactions when weighed against the complexity thus introduced.

In contrast to pure fluids, binary fluid–fluid phase equilibria exhibit most of the phenomena found in multicomponent mixtures. The relatively simple binary fluid phase equilibria therefore provide a practically useful basis for generalization of phase equilibrium principles (38), and are suitable for rationalizing the phase behavior-related phenomena typical of multicomponent reaction systems. However, note that phase equilibria are not necessarily reached in a flow reactor. Nevertheless such considerations are a valuable guide for the interpretation of the role of phase behavior in catalytic performance. Binary diagrams can be described by three dimensions and correspondingly be depicted in, e.g., p,T,x diagrams (pressure, temperature, composition). In weighing model accuracy against complexity, we propose to describe the phase behavior of reaction mixtures by binary fluid phase equilibria.

Even for binary fluid mixtures, phase diagrams reveal a great variety (10). To comprehensively discuss the phenomena encountered in such systems, it is of advantage to classify the various types of topologies. The classification used here is that introduced by Scott and van Konynenburg (39, 40). They predicted qualitatively five types of binary fluid phase diagrams by applying the empirical van der Waals equation of state to binary mixtures and recognized a sixth type empirically found in binary systems.

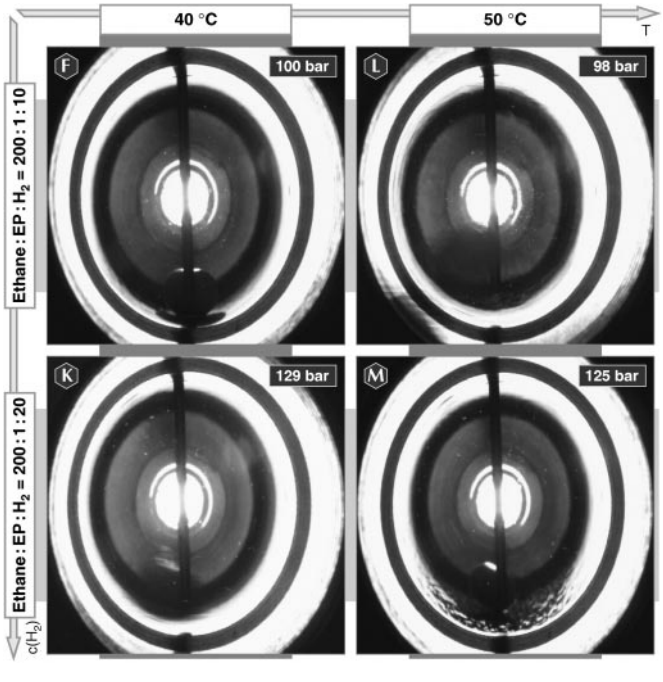

FIG. 13. Matrix of interlaced video images of the view cell showing the dependence of phase behavior on temperature and H_2 concentration. The reaction mixture consists of one phase at the conditions applied in (F), (K), and (L). An increase in temperature from conditions (K) or an increase in H_2 concentration from conditions (L) resulted in condensation of a new liquid EP-rich phase in (M) well above the critical values of ethane. For an explanation of the general features of the snapshots cf. Fig. 3.

The phase behavior of our reaction system can be understood in terms of immiscibility of the EP-rich and ethane-rich dense phases at higher temperatures, interfering with the gas–liquid critical line of the ethane-rich phases. It can be approached in the parameter range considered using a binary fluid phase diagram of type IV or V as a model. Binary mixtures conforming to types IV and V reveal complete miscibility of liquid phases at intermediate temperatures with the presence of a region of liquid–liquid immiscibility up to higher temperatures and thus interference with the gas–liquid critical line and the addition of a low-temperature liquid–liquid immiscibility in type IV. Figure 14 shows qualitatively an axonometry of the higher-temperature section of phase diagrams found in type IV and V binary mixtures. The isopleth at composition x_m in this diagram shows the same phase topology as found in the hydrogenation reaction mixture—self-evidently, apart from a higher degree of freedom for the three-phase equilibria found in the five-component mixture examined. The change in phase behavior with pressure in the temperature range 20–50°C (Fig. 2) may be well approximated by that of the binary model, as illustrated in Fig. 15. The binary fluid model embeds the experimentally observed phase behavior into a broader context. It ameliorates the qualitative understanding of the multicomponent phenomena observed, such as the difference in phase behavior observed at 30 and 40°C (Fig. 2), or the critical merging of the ethane-rich phases at around 40°C. Furthermore, it provides a feasible basis for extrapolation of the observed phase behavior to other temperatures and pressures, a prerequisite for the rational design of further experiments.

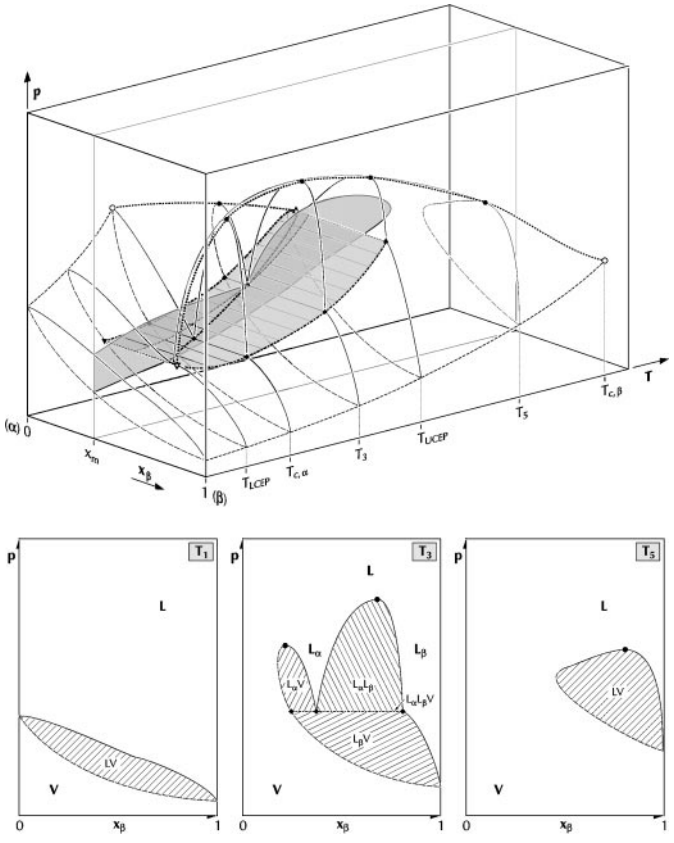

FIG. 14. Qualitative axonometry and corresponding intersections of the high-temperature section of a binary mixture showing type IV or type V phase behavior. α, Component of higher volatility; β, component of lower volatility; L, liquid phase; L_i, liquid phase rich in component i; V, gaseous (vapor) phase. Combinations of L, L_i, and V denote equilibria of mutually saturated phases and are emphasized by differing crosshatched filling of the corresponding two-phase area. Full line (in intersections): bubble-point line; dashed line (in intersections): dew-point line. (○) Critical point of the pure component; (●) mixture critical point (gas–liquid or liquid–liquid); (△) upper critical endpoint (UCEP); (▽) lower critical endpoint (LCEP); (◆) parameters of phases in equilibrium in $L_\alpha L_\beta V$ equilibrium shown in intersections. Note that the three-phase equilibrium $L_\alpha L_\beta V$ appears as a plane perpendicular to the p, T plane in p, T, x space. The isopleth at $x_\beta = x_m$ shows the same phase topology as found in the reaction mixture in the parameter range observed (see Fig. 15 right).

Interpretation of EP Hydrogenation on the Basis of Phase Behavior

The number and nature of coexisting phases during EP hydrogenation exhibited significant changes in the temperature, pressure, and H_2 concentration range examined. The observed variations in reaction rate and ee (Figs. 4, 6–9) may well be interpreted on the basis of this phase behavior study.

A dramatic effect of H_2 concentration on the reaction rate has been achieved by varying the overall density (Fig. 6). In the low-density region, where the EP-rich liquid phase coexists with the ethane-rich gas phase, EP is hydrogenated predominantly in the liquid phase. In contrast, at high overall density the reaction is confined to the ethane-rich, liquid or "supercritical" single phase. The predominant locus of reaction thus changes from the liquid EP-rich phase at low overall density to the dense (liquid or "sc") ethane-rich phase at high overall density. At high H_2 concentrations, this transition apparently occurs smoothly with increasing pressure (see Fig. 6). At low H_2 concentration, however, the hydrogenation of EP in the EP-rich liquid phase is relatively slow due to H_2 mass-transport limitations in the EP-rich liquid phase. The shift of the hydrogenation reaction to the ethane-rich dense phase with increasing pressure eliminates the mass-transport limitation, as reflected in the remarkable increase in EP conversion where single-phase conditions are reached.

There is a generally observed trend that increasing pressure (density) accelerates the reaction (see Fig. 6). This correlation can be traced to a faster hydrogenation reaction in the ethane-rich dense phase and/or an increase in residence time in the catalyst bed. The almost constant EP conversion, independent of pressure, at 50°C and high H_2 concentration (Fig. 7) can be attributed to another effect: with increasing H_2 availability and temperature, an

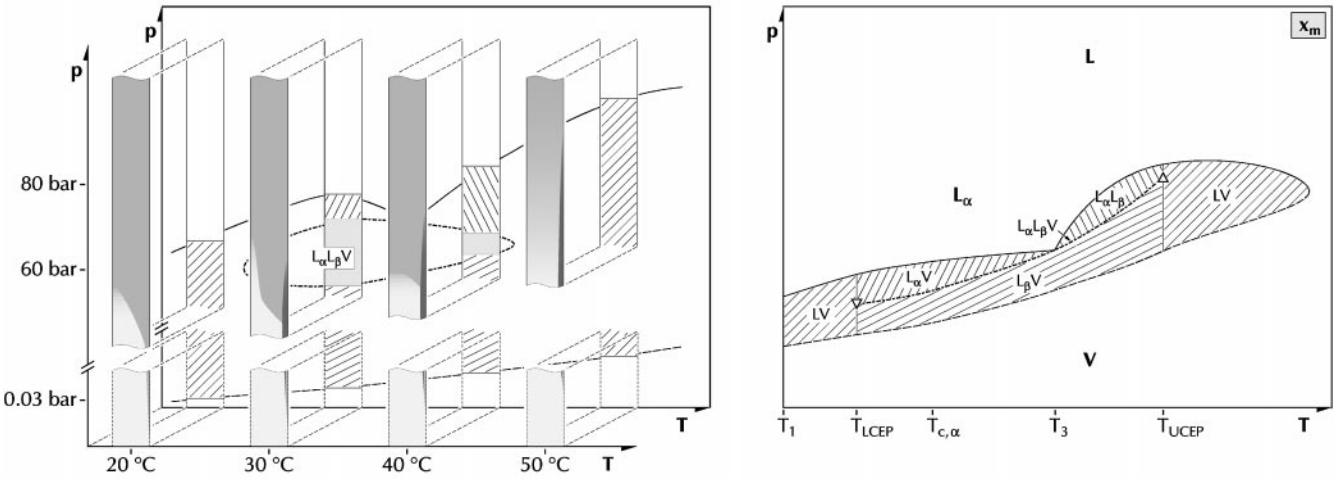

FIG. 15. Number and nature of phases in the hydrogenation reaction mixture (left), and the isopleth at composition x_m in the binary fluid mixture phase diagram used to model the phase behavior of the reaction (right; axonometry of the corresponding phase diagram is given in Fig. 14). Note the similarity in the phase behavior of the binary model and reaction mixture, apart from the degree of freedom for the three-phase liquid–liquid vapor equilibrium. α, Component of higher volatility; β, component of lower volatility; L, liquid phase; L_i, liquid phase rich in component i; V, gaseous (vapor) phase. Combinations of L, L_i, and V denote equilibria of mutually saturated phases and are emphasized by differing crosshatched filling of the corresponding two-phase area. The dewpoints for the reaction system (bottom left) have been estimated on basis of the vapor pressure of EP calculated from a two-parameter corresponding state equation (46) using the ambient boiling point and the critical temperature and pressure (calculated in accord using the Ambrose method as well as the Joback modification of Lyderson's method (46)) as a reference.

acceleration of the competing hydrogenation of the aromatic ring system of CD is expected. This transformation leads to weaker adsorption of the modifier on the Pt surface and, thus, to a loss of its enantio-differentiating ability (36, 41). Since CD not only provides the chiral information for EP hydrogenation but also accelerates the reaction (42–44), consumption of the major part of CD should have a negative effect on the hydrogenation rate. A similar negative effect can also be caused by temperature-induced changes in the adsorption mode of CD, as discussed in the context of Fig. 10.

The variations of enantioselectivity as a function of density (and conversion) have to be attributed to several overlapping effects. Higher enantioselectivity is expected in the ethane-rich dense phase due to stabilization of a favorable conformation of CD in the strongly apolar medium (45). Elimination of H_2 transport limitation in the dense ("supercritical") phase leads to higher actual surface hydrogen concentration, which in turn has a positive influence on the ee (13, 34). Acceleration of the competing hydrogenation of the aromatic ring system of CD is expected with increasing H_2 availability and temperature. Unfavorable adsorption of CD on Pt at higher temperature also diminishes the ee. Superposition of these effects leads to an increase in ee with increasing pressure at low H_2 concentration and temperature, whereas the opposite trend is established at higher H_2 concentration and temperature. These effects may lead to more complex variations as indicated by the bell-shaped ee conversion correlation in Fig. 9.

As illustrated above, the changes in reaction rate and ee during the enantioselective hydrogenation of EP can be interpreted with the knowledge obtained in the study of phase behavior of the ethane/H_2/EP system.

A comparison with the pertinent literature shows that the complexity of phase behavior—comprising the changes in composition of the phases—is often not contemplated sufficiently in the interpretation of high-pressure reactions. Without investigation of the phase behavior, striking changes in rate and selectivity are frequently attributed to an "expected" transition from two-phases to one-phase, i.e., the appearance of a single "sc" phase. Although in the present literature the necessity of studying the phase behavior of a multicomponent system is widely accepted, relatively little effort is made to experimentally confirm the phase behavior under reaction conditions. Description of the system's phase behavior with the phase behavior topology of a pure fluid does not take into account the possible changes in phase composition (and, correspondingly, surface concentration on a heterogeneous catalyst). It leads to an unacceptable oversimplification of the system under consideration. It has been shown that, in contrast to pure fluids, the phase diagram of binary systems is a very useful and appropriate tool for rationalizing the phase behavior of multicomponent systems.

From a technical point of view it is important that the process in "supercritical" ethane facilitates an easy and complete separation of the solvent from the reactants and products by simple expansion of the reaction mixture at the reactor outlet.

CONCLUSIONS

We have shown the feasibility of heterogeneously catalyzed continuous enantioselective hydrogenation of an α-ketoester in dense ("supercritical") ethane. Very high rates and good enantioselectivity were achieved by continuous dosing of small amounts of the chiral modifier CD, though optimization of the reaction conditions was not attempted. Elimination of the liquid–gas phase boundary in the reaction system at higher fluid density resulted in a significant enhancement of reaction rate only at low hydrogen concentrations. Generally, high fluid density increased reaction rate, whereas the effect on ee was less beneficial. Changes in the composition of the reaction mixture with conversion had little effect on the phase behavior in the system ethane, ethyl pyruvate, ethyl lactate, H_2.

Experiments performed in the temperature range up to 140°C showed that enantioselectivity drops strongly, whereas the reaction rate did not increase as expected from an Arrhenius-type behavior. This phenomenon is attributed to temperature-induced changes in the adsorption mode of CD and the partial hydrogenation of the quinoline moiety.

The study confirms that unambiguous interpretation of the sometimes striking changes in rate and selectivity of high-pressure reactions requires a careful analysis of the phase behavior under reaction conditions. The observed effects in systems far from a critical point have to be interpreted on the basis of this analysis, contemplating the unique combination of liquid-like and gas-like qualities for phases of intermediate density ("supercritical" phases). The complex phenomena inherent to multicomponent systems are absent in pure fluids, which difference explains why the solvent is an inappropriate model for the phase behavior of a reaction mixture. The combined catalytic and physicochemical study of EP hydrogenation demonstrates that the phase behavior of binary systems is an ideal guide for understanding high-pressure multicomponent reactions, particularly when weighing model accuracy against complexity.

ACKNOWLEDGMENTS

Financial support by the Swiss National Science Foundation and the Swiss Kommission für Technologie und Innovation (KTI) is gratefully acknowledged.

REFERENCES

1. Jessop, P. G., Ikariya, T., and Noyori, R., *Chem. Rev.* **99**, 475 (1999).
2. Brennecke, J. F., and Chateauneuf, J. E., *Chem. Rev.* **99**, 433 (1999).
3. Darr, J. A., and Poliakoff, M., *Chem. Rev.* **99**, 495 (1999).
4. Jessop, P. G., and Leitner, W., (Eds.), "Chemical Synthesis Using Supercritical Fluids." Wiley–VCH, Weinheim, 1999.
5. Baiker, A., *Chem. Rev.* **99**, 453 (1999).
6. Savage, P. E., *in* "Handbook of Heterogeneous Catalysis" (G. Ertl, H. Knözinger, and J. Weitkamp, Eds.), Vol. 3, p. 1339. Wiley–VCH, Weinheim, 1997.
7. Kiran, E., and Levelt Sengers, J. M. H. (Eds.), "Supercritical Fluids: Fundamentals for Application." Kluwer Academic, Dordrecht, 1994.
8. Wandeler, R., and Baiker, A., *CATTECH* **4**, 34 (2000).
9. Subramaniam, B., and McHugh, M. A., *Ind. Eng. Chem. Process Des. Dev.* **25**, 1 (1986).
10. Rowlinson, J. S., and Swinton, F. L., "Liquids and Liquid Mixtures," 3rd ed. Butterworth, London, 1982.
11. King, M. B., "Phase Equilibrium in Mixtures." Pergamon Press, Oxford, 1969.
12. Sun, Y., Wang, J., LeBlond, C., Landau, R. N., and Blackmond, D. G., *J. Catal.* **161**, 759 (1996).
13. Blaser, H. U., Jalett, H. P., Müller, M., and Studer, M., *Catal. Today* **37**, 441 (1997).
14. Baiker, A., and Blaser, H. U., *in* "Handbook of Heterogeneous Catalysis" (G. Ertl, H. Knözinger, and J. Weitkamp, Eds.), Vol. 5, p. 2422. Wiley–VCH, Weinheim, 1997.
15. Wells, P. B., and Wilkinson, A. G., *Top. Catal.* **5**, 39 (1998).
16. Bönnemann, H., and Braun, G. A., *Chem.-Eur. J.* **3**, 1200 (1997).
17. Augustine, R. L., and Tanielyan, S. K., *J. Mol. Catal. A* **118**, 79 (1997).
18. Farkas, G., Fodor, K., Tungler, A., Màthé, T.,Tòth, G., and Sheldon, R. A., *J. Mol. Catal. A* **138**, 123 (1999).
19. Margitfalvi, J. L., Talas, E., and Hegedüs, M., *Chem. Commun.*, 645 (1999).
20. Bartok, M., Felföldi, K., Török, B., and Bartok, T., *Chem. Commun.*, 2605 (1998).
21. Baiker, A., *J. Mol. Catal. A* **115**, 473 (1997).
22. Baiker, A., *J. Mol. Catal. A* **163**, 203 (2000).
23. Török, B., Felföldi, K., Szakonyi, G., Balazsik, K., and Bartok, M., *Catal. Lett.* **52**, 81 (1998).
24. Zuo, X., Liu, H., and Liu, M., *Tetrahedron Lett.* **39**, 1941 (1998).
25. Minder, B., Mallat, T., Pickel, K. H., Steiner, K., and Baiker, A., *Catal. Lett.* **34**, 1 (1995).
26. Wandeler, R., Künzle, N., Schneider, M. S., Mallat, T., and Baiker, A., *Chem. Commun.* **7**, 673 (2001).
27. Crampon, C., Charbit, G., and Neau, E., *J. Supercrit. Fluids* **16**, 11 (1999).
28. Wandeler, R., and Baiker, A., *Chimia* **53**, 566 (1999).
29. Wandeler, R., and Baiker, A., *in* "Virtuelle Instrumente in der Praxis:-Automation" (R. Jamal and R. Heinze, Eds.), p. 75. VDE-Verlag, Berlin, 2000.
30. Mallat, T., Frauchiger, S., Kooyman, P. J., Schürch, M., and Baiker, A., *Catal. Lett.* **63**, 121 (1999).
31. Ferri, D., Bürgi, T., Borszeky, K., Mallat, T., and Baiker, A., *J. Catal.* **193**, 139 (2000).
32. Künzle, N., Hess, R., Mallat, T., and Baiker, A., *J. Catal.* **186**, 239 (1999).
33. Schürch, M., Schwalm, O., Mallat, T., Weber, J., and Baiker, A., *J. Catal.* **169**, 275 (1997).
34. Mallat, T., Bodnar, Z., Minder, B., Borszeky, K., and Baiker, A., *J. Catal.* **168**, 183 (1997).
35. Evans, T., Woodhead, A. P., Gutiérrez-Sosa, A., Thornton, G., Hall, T. J., Davis, A. A., Young, N. A., Wells, P. B., Oldman, R. J., Plashkevych, O., Vahtras, O., Ågren, H., and Carravetta, V., *Surf. Sci.* **436**, L691 (1999).
36. LeBlond, C., Wang, J., Liu, J., Andrews, A. T., and Sun, Y.-K., *J. Am. Chem. Soc.* **121**, 4920 (1999).
37. Chrastil, J., *J. Phys. Chem.* **86**, 3016 (1982).

38. McHugh, M. A., and Krukonis, V. J., *in* "Supercritical Fluid Extraction: Principles and Practice," 2nd ed., p. 27. Butterworth–Heinemann, Boston, 1994.
39. Scott, R. L., and van Konynenburg, P. H., *Discuss. Faraday Soc.* **49**, 87 (1970).
40. van Konynenburg, P. H., and Scott, R. L., *Philos. Trans. R. Soc. London, Ser. A* **298**, 495 (1980).
41. Blaser, H. U., Jalett, H. P., Monti, D. M., Baiker, A., and Wehrli, J. T., *Stud. Surf. Sci. Catal.* **67**, 147 (1991).
42. Margitfalvi, J. L., Minder, B., Talas, E., Botz, L., and Baiker, A., *Stud. Surf. Sci. Catal.* **75**, 2471 (1993).
43. Bond, C., Meheux, P. A., Ibbotson, A., and Wells, P. B., *Catal. Today* **10**, 371 (1991).
44. Garland, M., and Blaser, H. U., *J. Am. Chem. Soc.* **112**, 7048 (1990).
45. Bürgi, T., and Baiker, A., *J. Am. Chem. Soc.* **120**, 12920 (1998).
46. Reid, R. C., Prausnitz, J. M., and Poling, B. E., "The Properties of Gases & Liquids," 4th ed., p. 742. McGraw–Hill, New York, 1988.